Multiscale neural connectivity during human sensory processing in the brain

Vladimir A. Maksimenko,[1] Anastasia E. Runnova,[1] Nikita S. Frolov,[1] Vladimir V. Makarov,[1] Vladimir Nedaivozov,[1] Alexey A. Koronovskii,[2] Alexander Pisarchik,[3,1] and Alexander E. Hramov[1,2]

[1]*Yuri Gagarin State Technical University of Saratov, REC "Artificial Intelligence Systems and Neurotechnologies", Saratov, 410054, Russia*

[2]*Saratov State University, Faculty of Nonlinear Processes, Saratov, 410012, Russia*

[3]*Technical University of Madrid, Campus Montegancedo, E-Madrid 28223, Spain*

(Received 19 February 2018; revised manuscript received 2 April 2018; published 15 May 2018)

Stimulus-related brain activity is considered using wavelet-based analysis of neural interactions between occipital and parietal brain areas in alpha (8–12 Hz) and beta (15–30 Hz) frequency bands. We show that human sensory processing related to the visual stimuli perception induces brain response resulted in different ways of parieto-occipital interactions in these bands. In the alpha frequency band the parieto-occipital neuronal network is characterized by homogeneous increase of the interaction between all interconnected areas both within occipital and parietal lobes and between them. In the beta frequency band the occipital lobe starts to play a leading role in the dynamics of the occipital-parietal network: The perception of visual stimuli excites the visual center in the occipital area and then, due to the increase of parieto-occipital interactions, such excitation is transferred to the parietal area, where the attentional center takes place. In the case when stimuli are characterized by a high degree of ambiguity, we find greater increase of the interaction between interconnected areas in the parietal lobe due to the increase of human attention. Based on revealed mechanisms, we describe the complex response of the parieto-occipital brain neuronal network during the perception and primary processing of the visual stimuli. The results can serve as an essential complement to the existing theory of neural aspects of visual stimuli processing.

DOI: 10.1103/PhysRevE.97.052405

I. INTRODUCTION

Analysis of the dynamics of the neural brain network by consideration of electroencephalograms (EEG) or magnetoencephalograms (MEG) is very important for understanding the sensory and cognitive functions of the brain. Many studies have shown the relationship between the electrical activity of brain and complex psychophysiological processes such as alertness [1], arousal [2], attention [3], memory [4], and executive functions [5]. Among these tasks, analysis of brain activity related to processing of visual stimuli is one of the most interesting and actively studied in modern science [6–8].

There are a lot of works addressed to the study of EEG signatures associated with visual perception. In particular, the influence of the oscillatory phase of EEG on perception was studied in [9,10], influence of the EEG energy was studied in [11], and interaction between different brain rhythms during perception was considered in [12].

One of the effective approaches to study the properties of visual perception is the use of the stimulus intensity value in the vicinity of a threshold. The threshold value can be defined as the value of stimulus intensity, at which each subject could detect 50% of the presented stimuli. This approach was used in [13] for studying of EEG spectral properties during visual detection performance. It was shown that alpha frequency band power decreased in occipital area during detection of the stimuli.

Another approach is the use of more complex stimuli which along with simple detection require their classification based on brief analysis of their structure. In this context the threshold parameter reflects the complexity of stimuli classification. This approach was recently used in [14] where ambiguous images were used as the stimuli. It was shown that the additional task of the stimuli classification induces additional change of the spectral properties of occipital EEG: Along with decrease in power of alpha rhythm there is increase of beta frequency activity.

Along with the effect of stimulus properties on the perceptive process the condition of the observer is known to affect the EEG spectral properties. In particular, the effect of the human factor on the perception was analyzed by considering two groups of subjects with an initially different degree of motivation. It was shown that the human factor, along with the properties of the stimuli affect the structure of occipital and parietal EEG [14].

According to the existing results the time frequency structure of occipital and parietal EEG reflects different properties of human sensory processing. These properties were extracted with the help of event-related potential (ERP) analysis [13], time frequency analysis [14], and methods of artificial intelligence and machine learning [15]. At the same time, the structure of the connectivity between neural ensembles belonging to these parts of the brain is poorly understood. Recent studies, however, report that the perceptual process is associated with stimulus-induced visual cortical networks [16] and, moreover, neural interactions play a key role in other processes, including arousal, attentional selection, and working memory [17]. It can be expected that analysis of the sensory processing in the brain related to the visual stimuli perception based on the consideration of connectivity on different timescales within a distributed cortical network will complement the results of time-frequency analysis and allow one to deeply understand

the neural mechanisms associated with processing of visual information [18–20].

In the current work we consider brain activity related to processing of visual stimuli (stimulus-related activity) based on analysis of interactions between the neural structures, belonging to occipital and parietal brain areas in alpha (8–12 Hz) and beta (15–30 Hz) frequency bands. We show that perception of visual stimuli induces brain response resulted in different ways of parieto-occipital interactions in these bands and describe the complex response of the parieto-occipital brain network during the perception and primary processing of the visual stimuli.

II. EXPERIMENTS AND EEG DATA PROCESSING METHODS

A. Experimental procedure

Twelve healthy subjects (males and females) between the ages of 20 and 43 with normal or corrected-to-normal visual acuity were chosen from the students and staff for the participation in the experimental researches. All of them provided informed written consent before participating in the experiment. The experimental studies were performed in accordance with the Declaration of Helsinki and approved by the local research ethics committee of the Yuri Gagarin State Technical University of Saratov.

The Necker cube [21] was used as the visual stimuli. Such an ambiguous stimulus is a popular object of many psychological experiments [22–24] and theoretical models [24–26]. It represents itself as a cube with transparent faces and visible edges; an observer without any perception abnormalities sees the Necker cube as a three-dimensional (3D) object due to the specific position of the cube's edges. Bistability in perception consists of the interpretation of this 3D object to be either left or right oriented depending on the contrast of different inner edges of the cube. The contrast $I \in [0,1]$ of the three middle lines centered in the left middle corner was used as a control parameter. The values $I = 1$ and $I = 0$ correspond, respectively, to 0 (black) and 255 (white) pixels' luminance of the middle lines. Therefore, we can define a contrast parameter as $I = y/255$, where y is the brightness level of the middle lines using the 8-bit grayscale palette. Using the ambiguous images as visual stimuli leads to an increase in the alertness of the subjects [14].

The whole experiment lasted around 50 min for each participant, including short recordings (∼300 s) of the brain background activity before and after the stimuli presentation. During experimental sessions, the cubes with predefined values of I [chosen from the set, illustrated in Fig. 1(a)] were randomly presented 400 times (each cube with a particular contrast was presented about 60 times). Structure of the experimental session is shown schematically in Fig. 1(b). Each ith stimulus was presented for the time interval τ_i, the next $(i+1)$th image was presented after time interval γ_i. In order to reduce "memory" effect, the length of the stimulus exhibition τ was varied in the range 1–1.5 s. Moreover, a random variation of the control parameter I also prevented the perception stabilization. Lastly, to draw away the observer's attention and make the perception of the next Necker cube independent of

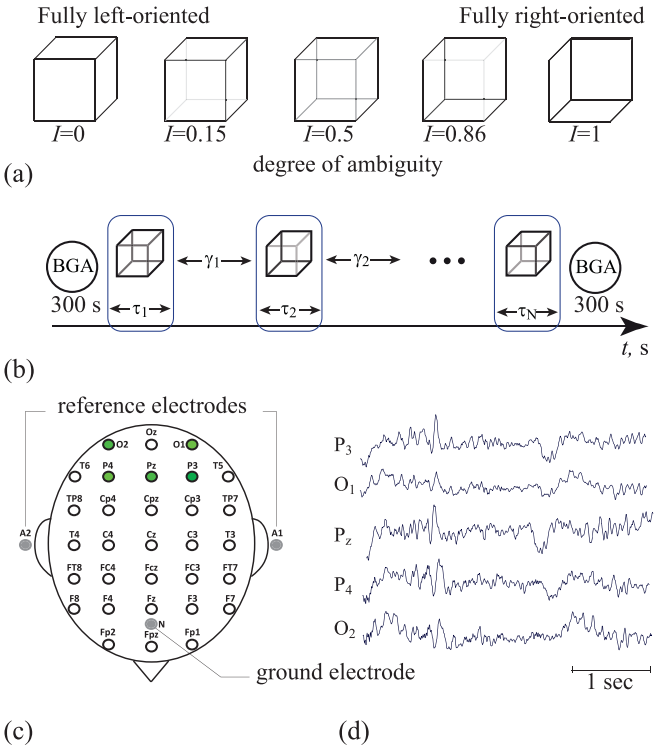

FIG. 1. (a) The set of visual stimuli (Necker cubes) with the different degree of ambiguity I. (b) Schematic illustration of the experimental sessions. τ_i is the time interval for which the ith cube is presented, γ_i is the interval between the ith and the $(i+1)$th presentation, and BGA defines sessions where background EEG activity is recorded. (c) EEG layout with marked reference and ground electrodes. (d) Typical set of EEG traces, associated with the visual stimulus-related brain activity.

the previous one, different abstract pictures were exhibited for about $\gamma = 5.0$–5.5 s between subsequent demonstrations of the Necker cube images. All participants were instructed to press either the left or right key depending on their first impression of the cube orientation at each presentation.

The electrical brain activity was recorded using the digital electroencephalographic recorder BE Plus LTM (EGI Medical Device Company, Italy) which provided simultaneous registration of up to 128 EEG channels with sample rate 8 kHz. The monopolar registration method and the classical extended ten-ten electrode system were used. To register EEG data we used cup adhesive Ag/AgCl electrodes placed on "TIEN-20" paste. Immediately before the experiment start, all the necessary procedures to increase the conductivity of the skin and reduce its resistance were carried out with the use of abrasive "NuPrep" gel. The impedances were monitored when the electrodes were installed and measured during experiments. Usually, the impedance values varied within 1 and 3 kΩ. The ground electrode N was located above the forehead and two reference electrodes $A_{1,2}$ were located on mastoids [see Fig. 1(c)]. The EEG signals were filtered by a band pass filter with cutoff points at 1 Hz (HP) and 100 Hz (LP) and a 50-Hz Notch filter. The BE Plus amplifier unit was used for amplification of the EEG signals. Preliminary EEG signal

processing was provided by the original software for EEG registration artifact suppression.

B. Time-frequency analysis

We analyzed the EEG signals recorded by five electrodes (O_1, O_2, P_3, P_4, P_z) [see Figs. 1(c) and 1(d)] placed on the standard positions of the ten-twenty international system [27], using the continuous wavelet transformation. The wavelet energy spectrum $E^n(f,t) = \sqrt{W_n(f,t)^2}$ was calculated for each EEG channel $X_n(t)$ in the frequency range $f \in [1,30]$ Hz. Here, $W_n(f,t)$ is the complex-valued wavelet coefficients calculated as

$$W_n(f,t) = \sqrt{f}\int_{t-4/f}^{t+4/f} X_n(t)\psi^*(f,t)dt, \tag{1}$$

where $n = 1,...,N$ is the EEG channel number ($N = 5$ is the total number of channels used for the analysis) and "*" defines the complex conjugation. The mother wavelet function $\psi(f,t)$ is the Morlet wavelet often used for analysis of neurophysiological data is defined as [28]

$$\psi(f,t) = \sqrt{f}\pi^{1/4} e^{j\omega_0 f(t-t_0)} e^{f(t-t_0)^2/2}, \tag{2}$$

where $\omega_0 = 2\pi$ is the wavelet parameter.

The wavelet energy spectrum was analyzed in two frequency bands: $\Delta f_\alpha = [8-12]$ Hz (alpha rhythm), and $\Delta f_\beta = [20-30]$ Hz (beta rhythm), corresponding to typical patterns of the visual stimulus-related neural activity.

For these frequency bands the corresponding wavelet energy values $E_\alpha(t)$ and $E_\beta(t)$ were calculated by averaging the spectral energy $E^n(f,t)$ over the corresponding alpha and beta bands as

$$E^n_{\alpha,\beta}(t) = \frac{1}{E^n_*(t)}\int_{\Delta f_{\alpha,\beta}} E^n(f',t)df', \tag{3}$$

where $E^n_*(t)$ is the energy value $E^n(f,t)$ averaged over the whole considered spectrum of the EEG signal,

$$E^n_*(t) = \int_{1\text{Hz}}^{30\text{Hz}} E^n(f',t)df'. \tag{4}$$

The values of the wavelet energy (3) calculated for the whole time of the experimental session were then averaged over the time segments τ_i and γ_i, related to the perception of ith visual stimuli, and over all EEG channels used for the analysis, as follows:

$$\langle E_{\alpha,\beta}\rangle_{\tau_i,\gamma_i} = \frac{1}{N}\sum_{n=1}^{N}\int_{\tau_i,\gamma_i} E^n_{\alpha,\beta}(t')dt'. \tag{5}$$

Finally, coefficients (5) were averaged over all M presentations,

$$\langle E_{\alpha,\beta}\rangle_{\tau,\gamma} = \frac{1}{M}\sum_{i=1}^{M}\langle E_{\alpha,\beta}\rangle_{\tau_i,\gamma_i}. \tag{6}$$

The values $\langle E_{\alpha,\beta}\rangle_{\tau,\gamma}$ were calculated for each experiment.

Along with the analysis of wavelet energy, the time frequency structure was considered based on wavelet "skeletons"—lines on the time-frequency plane, following the position of the spectral components with maximal wavelet energy. For every moment of time t^* we calculated the set of three skeletons, and described behavior of the first, second, and third maximal components of the wavelet spectrum. The skeleton of the first kind defined the value of frequency f_1^* for which the value of wavelet energy $E(f_1^*,t^*)$ reached maximal value for $t = t^*$. By analogy, skeletons of the second and third order were considered as the values of frequency $f_{2,3}^*$ for which the wavelet energy $E(f_{2,3}^*,t^*)$ reached the values next to the maximal.

C. Wavelet-based calculation of connectivity

Estimation of the coupling strength between different areas of brain based on the analysis of corresponding electrical or magnetic neural activity signals is a very important issue and many different techniques are applied. In particular, the different features of brain connectivity are revealed by means of Granger causality [29], nonlinear associations [30], recurrence-based methods [31], and entropy transfer methods [32]. In our study we use the wavelet-based approach. Continuous wavelet analysis is a well-established time series processing method, which allows one to extract the time-frequency structure of the nonstationary signals. In neuroscience wavelets are successively used for detection of the specific patterns of oscillatory activity [28]. In our recent work we have shown that wavelet analysis can be effectively used for the estimation of the coupling strength between the brain areas [33].

In the present research, the degree of interaction between the neural ensembles, whose collective dynamics is described by corresponded EEG signals is estimated via wavelet bicoherence. This method provides insight into nonlinear interactions of a different nature and is often applied for the analysis of biological signals [28,34] such as electrocardiogram [35], EEG [36], MEG [37], etc.

In order to calculate the degree of interaction between two dynamical systems, whose states are described by the variables $x_1(t)$ and $x_2(t)$, the corresponded complex-valued wavelet coefficients $W_1(f,t) = a_1 + ib_1$ and $W_2(f,t) = a_2 + ib_2$ should be considered.

Wavelet bicoherence is estimated based on the mutual wavelet spectrum $W_{1,2}(f,t)$ of the signals $x_1(t)$ and $x_2(t)$. Similarly to [38] the coefficients $\cos[\Delta\phi(f,t)]$ and $\sin[\Delta\phi(f,t)]$ represented as real and imaginary parts of the mutual wavelet spectrum can be calculated via the equations,

$$\cos[\Delta\phi(f,t)] = \frac{a_1(f,t)a_2(f,t) + b_1(f,t)b_2(f,t)}{\sqrt{a_1^2(f,t) + b_1^2(f,t)}\sqrt{a_2^2(f,t) + b_2^2(f,t)}} \tag{7}$$

and

$$\sin[\Delta\phi(f,t)] = \frac{b_1(f,t)a_2(f,t) - a_1(f,t)b_2(f,t)}{\sqrt{a_1^2(f,t) + b_1^2(f,t)}\sqrt{a_2^2(f,t) + b_2^2(f,t)}}. \tag{8}$$

Here $\Delta\phi(f,t) = \Delta\phi_2(f,t) - \Delta\phi_1(f,t)$ is the phase difference, calculated for considered signals $x_1(t)$ and $x_2(t)$ in the time-frequency domain. For further calculations values (7) and (8) have to be averaged over time intervals, for which the degree of coherence is considered.

In the current research, based on described formalism, we analyzed the degree of coherence between the different EEG signals, recorded in occipital and parietal brain areas during the background state and perception of visual stimuli. For the characterization of the stimulus-related brain state Eqs. (7) and (8) were averaged over time intervals $\tau_i = 1$ s for each individual perception. For the background state averaging was performed over time intervals, corresponding to background EEG. In order to exclude the effect of the interval length, background EEG was splitted into short intervals η_i (each of 1-s duration). As a result, for the ith interval (both for perception-related and background EEG) coefficients $(\cos[\Delta\phi(f)])_{\tau_i,\eta_i}$ and $(\sin[\Delta\phi(f)])_{\tau_i,\eta_i}$ were obtained as

$$(\cos[\Delta\phi(f)])_{\tau_i,\eta_i} = \int_{\tau_i,\eta_i} \cos[\Delta\phi(f,t)]dt, \qquad (9)$$

and

$$(\sin[\Delta\phi(f)])_{\tau_i,\eta_i} = \int_{\tau_i,\eta_i} \sin[\Delta\phi(f,t)]dt. \qquad (10)$$

Based on coefficients (9) and (10) the degree of coherence between the EEG signals on the ith interval was estimated based on the value of $\sigma(f)_{\tau_i,\eta_i}$, calculated as the amplitude of the mutual wavelet spectrum,

$$\sigma(f)_{\tau_i,\eta_i} = \sqrt{(\cos[\Delta\phi(f)])^2_{\tau_i,\eta_i} + (\sin[\Delta\phi(f)])^2_{\tau_i,\eta_i}}. \qquad (11)$$

The $\sigma(f)_{\tau_i,\eta_i}$ function takes the values from 0 to 1, containing the information about the degree of phase coherence of the two signals $x_1(t)$ and $x_2(t)$ for the particular frequency. Thereat $\sigma(f)_{\tau_i,\eta_i} = 0$ implies that there is no phase coherence at the current frequency, while for $\sigma(f)_{\tau_i,\eta_i} > 0$ coherence takes place.

Obtained values (11) were then averaged over M intervals and over frequency bands—alpha and beta ones. As a result, coefficients $\sigma^{\alpha,\beta}_{\text{per,bcg}}$, defined as the coherence between EEG signals during perception (per) and background activity (bcg) in alpha and beta frequency bands, were analyzed:

$$\sigma^{\alpha,\beta}_{\text{per,bcg}} = \frac{1}{M}\sum_{i=1}^{M}\int_{\alpha,\beta} \sigma(f)_{\tau_i,\eta_i} df. \qquad (12)$$

Finally, in order to estimate the stimulus-related brain activity changes in the degree of coherence, the differences $\Delta\sigma_{\alpha,\beta} = \sigma^{\alpha,\beta}_{\text{per}} - \sigma^{\alpha,\beta}_{\text{bcg}}$ were calculated for each pair of EEG recordings.

III. RESULTS AND DISCUSSION

Observation of the bistable Necker cube and its further interpretation as left or right oriented induces the stimulus-related response of the neuronal brain network. Such response is reflected in EEG data as the decrease of the amplitude of alpha rhythm (8–12 Hz oscillations) and increase of the amplitude of beta rhythm (15–30 Hz oscillations). Similar character of the brain activity is associated with the different types of perception, where changes in alpha activity are associated with the visual [39] or auditory attention [40] and changes of beta activity—with the cognitive activity, related to the procession of the stimuli [41] and shift of the brain to an attention state [42,43]. Role of the alpha–beta band activity in the perceptual process is also reported in Ref. [29] in the context of the information transfer in the visual areas.

In the case of the Necker cube such behavior is confirmed by the changes of the wavelet energy, calculated immediately before and after the beginning of the image presentation and averaged over alpha and beta frequency bands [see Fig. 2(a)]. Box-and-whiskers diagrams in Fig. 2(a) present the median of the wavelet energy values $\langle E_{\alpha,\beta}\rangle_\gamma$, calculated before the presentation of the image compared to the values $\langle E_{\alpha,\beta}\rangle_\tau$, calculated immediately after the presentation. One can see that energy of the alpha rhythm significantly decreases when the perception of the visual stimuli is started. At the same time, energy of the beta rhythm also exhibits increase, associated with visual perception. It should be noted that while decrease in alpha band energy is observed for all participants, increase

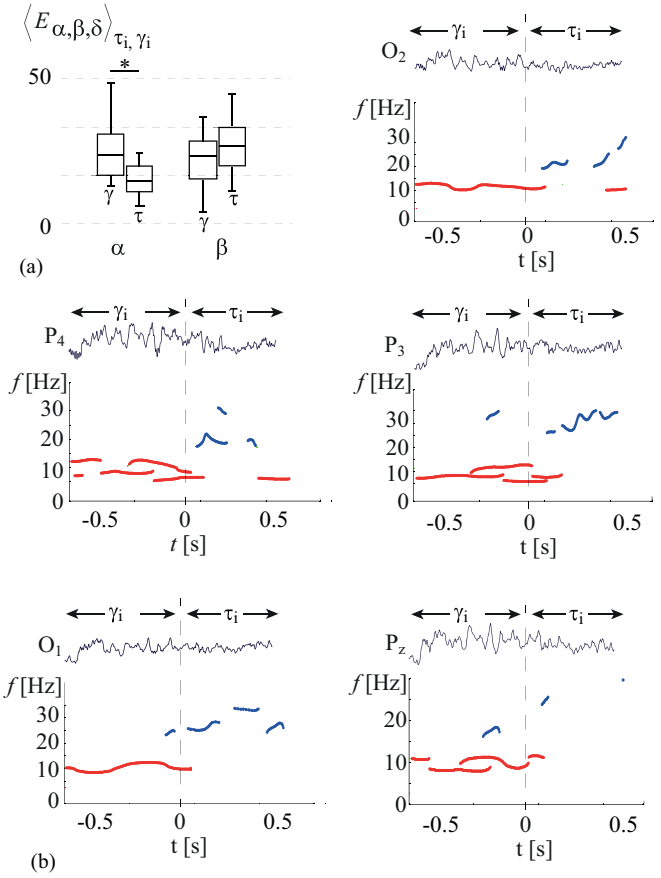

FIG. 2. Interplay between alpha and beta band activity. (a) (Left) Median of the mean alpha rhythm energy, calculated for the intervals, preceded (γ) and followed by (τ) the stimuli presentation ($n = 12$, $*p < 0.05$ via paired-sample t test); (right) median of the mean beta rhythm energy, calculated for the intervals, preceded (γ) and followed by (τ) the stimuli presentation ($n = 12$, $p = 0.09$ via paired-sample t test). (b) Typical EEG traces, associated with the perception of a single visual stimulus, and the wavelet skeletons, reflecting the location of the spectral components with maximal energy. Color of the curve defines the frequency band, in which the spectral component appears: red corresponds to alpha band, and blue to the beta band. Vertical dashed line defines the beginning of stimulus presentation.

of beta activity is observed in 60% of the subjects. Such inter-subject differences in the behavior of beta rhythm during the visual perception can be caused by human individual condition, e.g., his (her) ability to concentrate on the presented stimuli. According to recent work [14] significant brain response in beta frequency band is achieved in highly motivated subjects and in the case when complexity of the visual task is increased.

Obtained energy characteristics $\langle E_{\alpha,\beta}\rangle_{\tau,\gamma}$ are averaged over $N = 5$ EEG channels. From the one hand they reflect the contribution of the neural activity, recorded in the different parts of the occipital lobe, in generation of these types of brain rhythms [33]. From another hand, considered averaged values can reflect only the global trend in neural dynamics, but do not give information about local changes in the neural dynamics, i.e., processes of the interactions and coupling between the neural subnetworks, located in different areas of the occipital (or parietal) lobe.

In Fig. 2(b) the typical EEG traces, registered by these channels during the perception, are shown. With the EEG fragments one can see the location of the maximal spectral components. Lines show the evolution of three maximal spectral components. Color of the line reflects the appearance of the spectral component in alpha (red) and beta (blue) frequency bands. The spectral components, which appear in neither alpha nor beta frequency bands are excluded from the consideration.

First, one can see that when the stimuli have begun to be perceived by the subject the maximal spectral components change the location—they move from the range of alpha waves to the range of beta waves. This means that the corresponding neural ensembles start to be involved in the generation of the beta rhythm more intensively than in the generation of the alpha rhythm. It can be caused either by the increase of the number of neurons, participating in the rhythm generation or an increase of synchronization between them. In this case the energy of the oscillations, produced by the neurons moves mostly to the frequency band 15–30 Hz. Rhythms start to interplay: A decrease of alpha rhythm corresponds to an increase of beta rhythm and vice versa.

Second, similar stimulus-related behavior is observed in all considered EEG channels. This means that the oscillatory modes of the neural ensembles, located in the vicinity of the corresponding EEG electrodes in occipital and parietal lobes, begin to be synchronized by the external intervention—presentation of the visual stimuli.

Obviously, such a complex system as the network of occipital and parietal neurons responds to the external stimulus in a complicated way, which is implemented by the interplay between the different brain rhythms within one brain area (occipital or parietal) as well as between these two interconnected areas.

Understanding how the occipital and parietal brain structures interact is a very important issue [44]. In particular, an increase of parieto-occipital interactions was observed during the visual stimuli processing with the help of functional magnetic resonance imaging [45]. In Ref. [46] ERP analysis revealed parieto-occipital interactions, associated with processing of multisensory (auditory-visual) information. In Ref. [47] the participation of parietal and occipital areas in the perception of different visual features was analyzed based on the level of the inhibitory neurotransmitter.

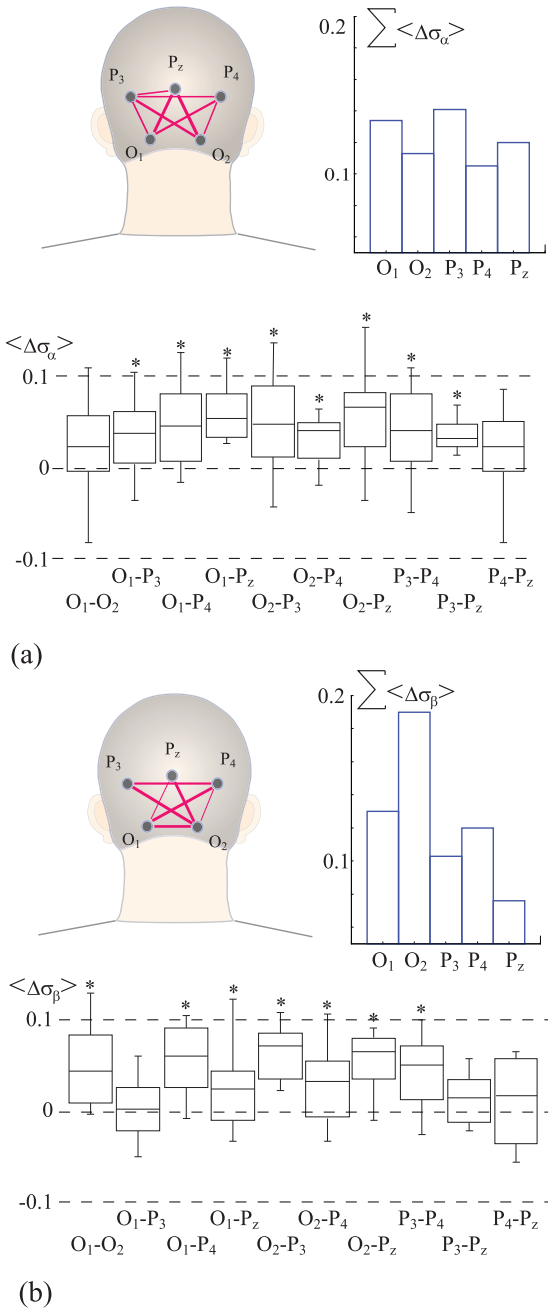

FIG. 3. Group analysis of stimulus-related differences in inter-channel interactions. (a) Alpha frequency band, (b) beta frequency band: box-and-whiskers diagrams show median of the difference between the degrees of coherence, calculated for stimulus-related and background EEG ($n = 12$, $*p < 0.05$ via paired-sample t test); histogram shows the sum change in the degree of interaction for each EEG channel; schematic visualization demonstrates the change in the degree of coherence by the width of line and excludes the links, for which such change is judged as insignificant.

In the current work the stimulus-related parieto-occipital interactions were studied based on the wavelet bicoherence. Degree of coherence was estimated between the pairs of occipital EEG in two frequency bands: 8–12 Hz and 15–30 Hz during the background activity (σ_{bcg}) and perception of the stimuli (σ_{per}). In Fig. 3 box-and-whiskers diagrams correspond to the

median of the difference between σ_{per} and σ_{bcg}, calculated for the group of 12 subjects in alpha (a) and beta (b) frequency bands. The symbol "*" defines the channel pairs for which the significant change ($p > 0.05$) is observed. Links between such pairs are shown schematically on the occipital and parietal lobes. The line width illustrates the mean value of $\Delta\sigma$ (degree of the change of the coupling strength between corresponded EEG traces, caused by the processing of the stimuli). One can see that in both alpha and beta frequency bands the majority of channel pairs demonstrate an increase of the coupling strength during the cube observation, which coincides with the results of functional magnetic resonance imaging [45]. It also coincides with [29], where the increase of interaction between areas of visual cortex has been observed across alpha and beta frequency ranges. However, in Refs. [29,48] such stimulus-related activity has been associated with the frequency band 10–30 Hz including both alpha and beta frequencies. At the same time, our results, similarly to [49,50], reveal the differences in alpha and beta activity. This represents itself as the difference in the structure of the links in these bands. In order to quantify these differences we have calculated the sum of $\Delta\sigma$ values, related to each EEG channel. This coefficient illustrates the change of the weight of each node (in our case the corresponded brain region), caused by the stimulus processing.

The values $\Delta\sigma$ are shown in Fig. 3 by the histograms. One can see that in the alpha band [Fig. 3(a)] $\Delta\sigma$ is distributed homogeneously within the occipital and parietal EEG channels. In the beta band [histogram in Fig. 3(b)], it is unlikely one can observe a sharp increase of $\Delta\sigma$ for occipital channel O2. This means that the alpha activity is produced by the network of interconnected brain regions, with the homogeneous structure of the links, which is similar to the structure, associated with background neural activity (but with the increased weights of the links). Beta activity is produced by the network, where one can see the formation of the hub in the occipital area, which plays key functional roles in inter-regional interactions. This result is in good agreement with an earlier work of Wróbel *et al.* [42] where the hypothesis about the leading role of beta oscillations in perception was put forward. The revealed impact of the occipital area can be explained by the leading role of this area in the perception of stimuli with different spatial orientation [47].

Having considered the stimulus-related change in the degree of coupling strength one can conclude the following: (i) Processing of visual stimuli results in the increase of the degree of coupling strength between EEG channels belonging to occipital and parietal lobes both in alpha and beta frequency bands; (ii) in alpha frequency band interaction between all EEG channels increases equally and one cannot extract the brain area where the increase of the inter-region coupling is the most pronounced; (iii) in the beta frequency band one can find occipital channel O2 which demonstrates a sharp increase of the coupling strength with other EEG channels. Obtained results confirm the formation and coexistence of different regimes of neuronal activity in different frequency bands. These regimes are characterized by a different structure of the links between brain areas, belonging to occipital and parietal lobes.

Along with the different oscillatory patterns, observed in different spectral bands of the occipital-parietal structure,

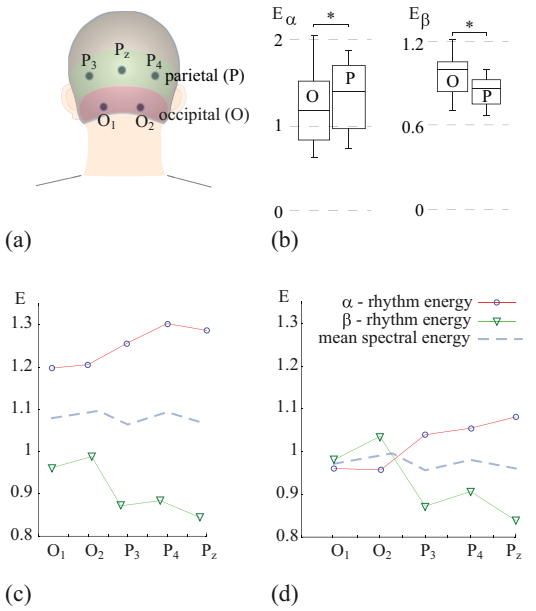

FIG. 4. Multiscale interaction between brain rhythms in occipital and parietal area. (a) Location of EEG electrodes in occipital and parietal brain lobes. (b) (Left) Median of the alpha rhythm energy, calculated based on occipital (O) and parietal (P) EEG ($n = 12$, $*p < 0.05$ via paired-sample t test); (right) median of the beta rhythm energy, calculated based on occipital (O) and parietal (P) EEG ($n = 12$, $*p < 0.05$ via paired-sample t test). (c) Mean energy of alpha and beta rhythms, calculated for each channel during background state. (d) Mean energy of alpha and beta rhythms, calculated for each channel during perception. Dashed lines show the mean spectral energy, calculated in 1- to 30-Hz frequency band.

differences exist in the neural dynamics in these particular brain areas. Having considered the ratio of the energy of alpha and beta rhythms, generated in these brain areas during the background state, one can see that alpha waves are generated more intensively in the parietal lobe, while the beta rhythm is generated more intensively in the occipital lobe. In Fig. 4(b) the box-and-whiskers plot shows the median of the wavelet energy, averaged over alpha and beta frequency bands in occipital (O) and parietal (P) areas ($*p < 0.05$ by paired-sample t test, $n = 12$). In Fig. 4(c) the values of wavelet energy, characterizing generation of alpha and beta rhythms during the background state, are shown for each EEG channel (presented data are averaged over 12 subjects). It can be seen that during the background state, despite the different intensity of the generation of alpha and beta rhythms in different channels, the difference between the energy of these rhythms is more pronounced. During the processing of the visual stimulus the situation is changed—in the occipital area (channels O1 and O2) beta activity starts to prevail; in the parietal area (channels P3, P4, and Pz) alpha activity is still more pronounced, but its energy becomes much less than during the background state [see Fig. 4(d)]. According to earlier EEG and functional magnetic resonance imaging (fMRI) study, such differences in the neural dynamics in the parietal and occipital areas can be associated with the existence of "visual" areas in the occipital lobe and "attentional" areas in the parietal lobe [51]. Taking into account Ref. [52], where the stimulus-related generation

of beta waves in the visual cortex has been observed, one can conclude that the occipital area first exhibits the excitation in the beta band and then causes the increase of beta-wave activity in the parietal region.

At the same time, for each channel (occipital and parietal) an increase of the generation of beta activity is accompanied by a decrease of the generation of the alpha rhythm.

One can propose that in the neural ensembles, located in the vicinity of the corresponding electrodes, during the background state most of the neurons are involved in generation of alpha activity, while a much smaller amount of neurons are acting in the beta frequency range. In the occipital area the size of the neural ensemble involved in generation of beta activity is larger than in the parietal lobe which can be caused by excitation of the "visual" center by constant incoming visual information. During the perception of ambiguous stimuli, the income of external visual information is greatly increased. In this case the large amount of neurons in the occipital lobe shift to the generation of signals in the beta frequency range. Amplitude of alpha-wave activity in this region becomes much less [see Fig. 4(d)]. Then, according to the results of the connectivity analysis, in the beta frequency band the occipital lobe starts to play a leading role in the dynamics of the occipital-parietal network. This leads to the increase of beta activity in the parietal area. An increase of beta activity in the occipital and parietal areas leads to a decrease of the energy of alpha activity in these regions. Such changes in the energy of alpha-wave activity is thereby observed in all EEG channels belonging to occipital and parietal brain areas. This in turn leads to the increase of the coupling strengths between the channels in these areas in the alpha band.

The features of stimulus-related brain activity are known to depend on the parameters of the stimuli. In particular, for the Necker cube the difference in the time-frequency structure is observed for different values of cube ambiguity I. For instance, in [14] the perception of the cubes with high ambiguity ($I \sim 0.5$) was shown to induce more pronounced increase of the spectral energy above 30 Hz. In the recent work [53] the artificial neural network trained to classify brain response associated with the perception of unambiguous cubes was shown to exhibit a sharp decrease in classification accuracy, when the degree of ambiguity became greater. In this respect one can expect that the coupling strength between the regions of the parieto-occipital brain network depend on the degree of image ambiguity. In order to verify this hypothesis, we have calculated the degree of interaction between the pairs of EEG channels during the perception of the Necker cubes with high ambiguity (HA) ($0.6 > I > 0.4$) and low ambiguity (LA) ($I > 0.8$ or $I < 0.2$) separately. For each pair we have then calculated difference $\Delta\sigma^{\mathrm{HA-LA}}$ between the obtained values. In Fig. 5 such differences are shown for 12 participants in beta (a) and alpha (b) frequency bands. One can see that in the alpha band the mean value of $\Delta\sigma^{\mathrm{HA-LA}}$ is mostly negative. This is evidence that in this band the increase of image ambiguity results in the decrease of interchannel interaction. In the beta frequency band some channel pairs are characterized by negative value of $\Delta\sigma^{\mathrm{HA-LA}}$, while for others $\Delta\sigma^{\mathrm{HA-LA}}$ is positive. One can see that significant difference $\Delta\sigma^{\mathrm{HA-LA}} > 0$ is observed for P3–P4, Pz–P4, and P3–O2 channel pairs as shown in the inserts in Fig. 5. This means that processing of

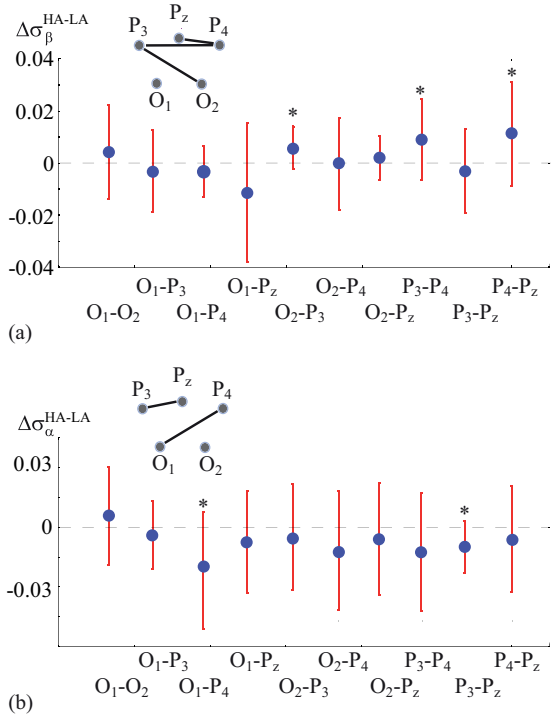

FIG. 5. Effect of image ambiguity. Difference between the degree of interchannel interaction (mean ± SD) calculated during the processing of the images with high ambiguity ($0.6 > I > 0.4$) and low ambiguity ($I > 0.8$ or $I < 0.2$) in beta (a) and alpha (b) frequency bands ($n = 12$, $*p < 0.05$ via paired-sample t test).

the images with high ambiguity increases human attention and, therefore, causes the increase of the neural interactions in the parietal lobe, where the "attentional" center is located [51].

IV. CONCLUSION

Human sensory processing in the brain related to the visual stimuli perception causes the increase of incoming visual information, and shifts the brain to the state of high attention. These processes induce the excitation of neural ensembles, belonging to the "visual" area (located in the occipital lobe) and the "attentional" area (located in the parietal lobe), and results in complex interactions on different timescales between these areas of the brain.

In the present work, based on time-frequency analysis and the study of wavelet coherence between occipital and parietal EEG we describe the scenario of stimulus-related brain response via the following way (see Fig. 6): (i) incoming visual information excites the neurons in the occipital lobe ("visual area") and makes them generate 15- to 30-Hz oscillations more intensively; (ii) the significance of the occipital area in the occipital-parietal network becomes greater. Neurons in this part of the brain, being excited by the external visual input affect the neurons in the parietal lobe ("attentional area") and they, in turn, start to be involved in the generation of oscillatory activity in the 15- to 30-Hz frequency band (1); (iii) increase in the amplitude of 15- to 30-Hz oscillations of the beta band in the occipital and parietal lobes results in the decrease of alpha band power since the majority of the neurons are shifted

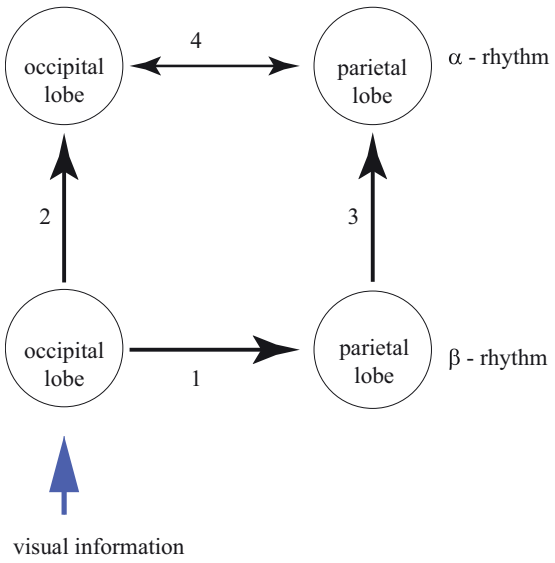

FIG. 6. Stimulus-related response of the parieto-occipital network: interaction between parietal and occipital brain areas (1,4), estimated via the wavelet bicoherence between corresponding EEG and interactions between alpha and beta band activity (2,3), and estimated for parietal and occipital EEG based on the wavelet energy and structure of wavelet skeletons.

to generate the high frequency beta rhythm (2,3). The latter causes the similarity in the behavior of the neural ensembles in the 8- to 12-Hz band, which is reflected in the increase of the interactions between the occipital and parietal areas, estimated for these frequencies (4). In the case when stimuli are characterized by a high degree of ambiguity, a greater increase of the interaction between interconnected areas in the parietal lobe is due to the increase of human attention.

Obtained results are in good agreement with earlier studies, describing the existence of "visual" and "attentional" areas and their operation at the 15- to 30-Hz frequency band, and demonstrating the increase of stimulus-related neural interactions in the alpha and beta bands; we believe the results can serve as a complement to the existing theory of neural aspects of visual stimuli processing.

ACKNOWLEDGMENTS

We would like to express our gratitude to the reviewer for comments and suggestions that have improved the article. This work has been supported by the Russian Science Foundation (Grant No. 17–72–30003).

[1] T.-P. Jung, S. Makeig, M. Stensmo, and T. J. Sejnowski, IEEE Trans. Biomed. Eng. **44**, 60 (1997).
[2] M. Balconi and C. Lucchiari, International Journal of Psychophysiology **67**, 41 (2008).
[3] N.-H. Liu, C.-Y. Chiang, and H.-C. Chu, Sensors (Basel) **13**, 10273 (2013).
[4] J. Onton, A. Delorme, and S. Makeig, Neuroimage **27**, 341 (2005).
[5] P. Sauseng, W. Klimesch, M. Schabus, and M. Doppelmayr, International Journal of Psychophysiology **57**, 97 (2005).
[6] Y. Wamain, A. Sahaï, J. Decroix, Y. Coello, and S. Kalénine, Biol. Psychol. **132**, 202 (2018).
[7] G. V. Kumar, T. Halder, A. K. Jaiswal, A. Mukherjee, D. Roy, and A. Banerjee, Frontiers in Psychology **7**, 1558 (2016).
[8] R. F. Helfrich, M. Huang, G. Wilson, and R. T. Knight, Proc. Natl. Acad. Sci. **114**, 9457 (2017).
[9] N. A. Busch, J. Dubois, and R. VanRullen, J. Neurosci. **29**, 7869 (2009).
[10] A. Milton and C. W. Pleydell-Pearce, Neuroimage **133**, 53 (2016).
[11] N. Shourie, J. Med. Signals Sens. **6**, 203 (2016).
[12] Y. Tu, Z. Zhang, A. Tan, W. Peng, Y. S. Hung, M. Moayedi, G. D. Iannetti, and L. Hu, Human Brain Mapping **37**, 501 (2016).
[13] T. Ergenoglu, T. Demiralp, Z. Bayraktaroglu, M. Ergen, H. Beydagi, and Y. Uresin, Cognit. Brain Res. **20**, 376 (2004).
[14] V. A. Maksimenko, A. E. Runnova, M. O. Zhuravlev, V. V. Makarov, V. Nedayvozov, V. V. Grubov, S. V. Pchelintceva, A. E. Hramov, and A. N. Pisarchik, PLoS ONE **12**, e0188700 (2017).
[15] A. E. Hramov, V. A. Maksimenko, S. V. Pchelintseva, A. E. Runnova, V. V. Grubov, V. Y. Musatov, M. O. Zhuravlev, A. A. Koronovskii, and A. N. Pisarchik, Front. Neurosci. **11**, 674 (2017).
[16] C. M. Lewis, C. A. Bosman, T. Womelsdorf, and P. Fries, Proc. Natl. Acad. Sci. **113**, E606 (2016).
[17] A. K. Engel and P. Fries, in *The Neurology of Consciousness*, 2nd ed. (Elsevier, Amsterdam, 2016), pp. 49–60.
[18] S. L. Fairhall and A. Ishai, Cereb. Cortex **17**, 2400 (2006).
[19] S. Peltier, R. Stilla, E. Mariola, S. LaConte, X. Hu, and K. Sathian, Neuropsychologia **45**, 476 (2007).
[20] J. Vezoli, A. Bastos, C. Bosman, J. Schoffelen, R. Oostenveld, P. D. Weerd, H. Kennedy, and P. Fries, Perception **42**, 143 (2013).
[21] L. N. Esq., The London, Edinburgh, and Dublin Philosophical Magazine and Journal of Science **1**, 329 (1832).
[22] J. Kornmeier, M. Pfäffle, and M. Bach, Journal of Vision **11**, 12 (2011).
[23] B. Mathes, D. Strüber, M. A. Stadler, and C. Basar-Eroglu, Neurosci. Lett. **402**, 145 (2006).
[24] A. N. Pisarchik, R. Jaimes-Reátegui, C. D. A. Magallón-García, and C. O. Castillo-Morales, Biol. Cybern. **108**, 397 (2014).
[25] A. N. Pisarchik, I. A. Bashkirtseva, and L. B. Ryashko, Eur. Phys. J.: Spec. Top. **224**, 1477 (2015).
[26] A. N. Pisarchik, I. Bashkirtseva, and L. Ryashko, Indian J. Phys. **91**, 57 (2017).
[27] E. Niedermeyer and F. L. da Silva, *Electroencephalography: Basic Principles, Clinical Applications, and Related Fields, Nonlinear Dynamics* (Lippincot Williams & Wilkins, Philadelphia, 2014).
[28] A. E. Hramov, A. A. Koronovskii, V. A. Makarov, A. N. Pavlov, and E. Sitnikova, *Wavelets in Neuroscience* (Springer, Berlin/Heidelberg, 2015).

[29] G. Michalareas, J. Vezoli, S. Van Pelt, J.-M. Schoffelen, H. Kennedy, and P. Fries, Neuron **89**, 384 (2016).
[30] F. L. da Silva, J. P. Pijn, and P. Boeijinga, Brain Topography **2**, 9 (1989).
[31] G. Ouyang, X. Li, C. Dang, and D. A. Richards, Clin. Neurophysiol. **119**, 1747 (2008).
[32] R. Vicente, M. Wibral, M. Lindner, and G. Pipa, J. Comput. Neurosci. **30**, 45 (2011).
[33] V. A. Maksimenko, A. Lüttjohann, V. V. Makarov, M. V. Goremyko, A. A. Koronovskii, V. Nedaivozov, A. E. Runnova, G. van Luijtelaar, A. E. Hramov, and S. Boccaletti, Phys. Rev. E **96**, 012316 (2017).
[34] K. Schiecke, M. Wacker, F. Benninger, M. Feucht, L. Leistritz, and H. Witte, IEEE Trans. Biomed. Eng. **62**, 1937 (2015).
[35] L. W. Sheppard, V. Vuksanović, P. McClintock, and A. Stefanovska, Phys. Med. Biol. **56**, 3583 (2011).
[36] M. Le Van Quyen, J. Foucher, J.-P. Lachaux, E. Rodriguez, A. Lutz, J. Martinerie, and F. J. Varela, J. Neurosci. Methods **111**, 83 (2001).
[37] V. Sakkalis, Comput. Biol. Med. **41**, 1110 (2011).
[38] A. Bandrivskyy, A. Bernjak, P. McClintock, and A. Stefanovska, Cardiovascular Engineering: An International Journal **4**, 89 (2004).
[39] P. Sauseng, W. Klimesch, W. Stadler, M. Schabus, M. Doppelmayr, S. Hanslmayr, W. R. Gruber, and N. Birbaumer, European Journal of Neuroscience **22**, 2917 (2005).
[40] J. J. Foxe and A. C. Snyder, Frontiers in Psychology **2**, 154 (2011).
[41] P. Sehatpour, S. Molholm, T. H. Schwartz, J. R. Mahoney, A. D. Mehta, D. C. Javitt, P. K. Stanton, and J. J. Foxe, Proc. Natl. Acad. Sci. **105**, 4399 (2008).
[42] A. Wróbel *et al.*, Acta Neurobiol. Exp. **60**, 247 (2000).
[43] M. Gola, M. Magnuski, I. Szumska, and A. Wróbel, International Journal of Psychophysiology **89**, 334 (2013).
[44] T. C. Sprague and J. T. Serences, Nat. Neurosci. **16**, 1879 (2013).
[45] I. Indovina and E. Macaluso, Magn. Reson. Imaging **22**, 1477 (2004).
[46] S. Molholm, W. Ritter, M. M. Murray, D. C. Javitt, C. E. Schroeder, and J. J. Foxe, Cognit. Brain Res. **14**, 115 (2002).
[47] C. Song, K. Sandberg, L. M. Andersen, J. U. Blicher, and G. Rees, J. Neurosci. **37**, 8929 (2017).
[48] E. A. Buffalo, P. Fries, R. Landman, T. J. Buschman, and R. Desimone, Proc. Natl. Acad. Sci. **108**, 11262 (2011).
[49] S. Haegens, H. Cousijn, G. Wallis, P. J. Harrison, and A. C. Nobre, Neuroimage **92**, 46 (2014).
[50] G. G. Gregoriou, S. Paneri, and P. Sapountzis, Brain Research **1626**, 165 (2015).
[51] H. Laufs, J. L. Holt, R. Elfont, M. Krams, J. S. Paul, K. Krakow, and A. Kleinschmidt, Neuroimage **31**, 1408 (2006).
[52] J. T. Schmiedt, A. Maier, P. Fries, R. C. Saunders, D. A. Leopold, and M. C. Schmid, J. Neurosci. **34**, 11857 (2014).
[53] A. E. Hramov, N. S. Frolov, V. A. Maksimenko, V. V. Makarov, A. A. Koronovskii, J. Garcia-Prieto, L. F. Antón-Toro, F. Maestú, and A. N. Pisarchik, Chaos: An Interdisciplinary Journal of Nonlinear Science **28**, 033607 (2018).